

Fine Structure of Polymer Networks As Revealed by Solvent Swelling

Ferenc Horkay

General Electric Corporate Research and Development, P.O. Box 8, Schenectady, New York 12301

Anne-Marie Hecht and Erik Geissler*

Laboratoire de Spectrométrie Physique, CNRS UMR5588, B.P. 87,
38402 St. Martin d'Hères Cedex, France

Received October 31, 1997

ABSTRACT: Measurements are reported of small-angle neutron scattering (SANS) from lightly cross-linked poly(vinyl acetate) gels swollen in good and Θ solvents. In all the solvent conditions investigated the scattering response can be described satisfactorily by two characteristic length scales: a thermodynamic correlation length ξ that is related to the osmotic swelling pressure and a larger distance Ξ that is governed by the range of the random elastic forces exerted by the cross-links. ξ decreases significantly as the overall polymer concentration increases; the static correlation length Ξ , however, decreases only weakly as the gels shrink. For samples in a good solvent undergoing uniaxial stretching, a butterfly pattern is observed which is also well described in terms of two length scales. In Θ conditions, however, this effect is masked by incipient phase separation in the gel in which the precipitated regions are elongated along the stretching direction.

Introduction

Small-angle neutron or X-ray scattering (SANS and SAXS) experiments reveal the structure of amorphous materials in the range of length scales between 1 and 100 nm. This resolution is of particular interest in the field of polymers, such as solutions and gels. In the simplest case of a dilute polymer solution, two length scales are required to describe the system: that of the local chemical architecture, i.e., the length of the repeating unit, and the radius of gyration R_G of the individual coils.¹ In more concentrated solutions, as the coils overlap they lose their individuality, and the thermodynamic properties are governed by another length scale, ξ , the correlation length between polymer segments.² In this overlapping (semidilute) regime, however, an additional length scale arises—the distance between entanglements along a given chain, which controls primarily the dynamic response through the plateau modulus of the solution.³ In a chemically cross-linked network, the situation is more complex: (i) the presence of cross-links imposes permanent constraints on the network chains; (ii) rearrangements of the polymer segments occur that depend on the details of the cross-linking procedure. These superstructures are detectable at high degrees of swelling, where they appear as concentrated regions embedded in a more dilute background. Neutron scattering is a powerful tool for revealing the spatial extent of these longer range supermolecular structures, which control the overall physical behavior of the network both in the dry and in the swollen state.^{4–8}

The aim of this article is to enquire into length scales required to describe the structure and thermodynamics of gels. To this end, we have performed small-angle neutron and X-ray scattering measurements on a set of poly(vinyl acetate) networks in a series of solvents of differing thermodynamic quality.

The discussion of the results is divided into three sections: one concerned with isopropyl alcohol at 52 and at 70 °C (Θ and moderately good solvents) and one

dealing with acetone, which, owing to its smaller molar volume, exerts a significantly higher osmotic pressure. In the third section, the effect of uniaxial stretching on the scattering behavior is discussed.

Theoretical Section

In a uniform polymer solution of volume fraction φ , the intensity of the scattered radiation of wavelength λ is given by⁹

$$I(Q) = (\rho_p - \rho_s)^2 \frac{kT\varphi^2}{K_{os}} S(Q) \quad (1)$$

where $Q = 4\pi n/\lambda \sin(\theta/2)$ is the transfer wave vector, n the refractive index, and θ the scattering angle. In eq 1, $(\rho_p - \rho_s)^2$ is the contrast factor between polymer and solvent, $K_{os} (= \varphi \partial \Pi / \partial \varphi)$, Π being the osmotic pressure of the solution) is the osmotic compressional modulus, and $S(Q)$ is the structure factor. For semidilute polymer solutions at small values of Q , $S(Q)$ is approximated² by an Ornstein–Zernicke line-shape function

$$S(Q) = \frac{1}{1 + Q^2 \xi^2} \quad (2)$$

where ξ is the polymer–polymer correlation length.

For a gel, the scattering intensity has been found to follow an expression of the form¹⁰

$$I(Q) = I_1(Q) + I_2(Q) \\ = (\rho_p - \rho_s)^2 \left[\frac{kT\varphi^2}{M_{os}} \frac{1}{1 + Q^2 \xi^2} + \right. \\ \left. 8\pi \Xi^3 \langle \delta \varphi^2 \rangle \frac{1}{(1 + Q^2 \Xi^2)^2} \right] \quad (3)$$

where the first term, analogous to eq 1, describes the thermodynamic response. The modulus M_{os} appearing in the denominator of this term is given by^{11,12} $M_{os} =$

$K_{\text{osgel}} + 4G/3$, where G is the elastic modulus of the gel and $K_{\text{osgel}} = \varphi \partial\omega/\partial\varphi$ is the osmotic modulus of the gel, ω being the swelling pressure. The second term describes static concentration fluctuations of mean-square amplitude $\langle\delta\varphi^2\rangle$ generated by random elastic strains in the gel; it is based on the theoretical expression of Debye and Bueche.¹³ The corresponding correlation length Ξ can therefore be expected to be of the order of the radius of gyration of a constituent polymer coil in the network. The gel is thus pictured as consisting of a set of coils that, owing to the forces exerted by the cross-links, are incompletely screened by the osmotic pressure, giving rise to excess scattering at low Q .

Experimental Section

PVAc gels were prepared using a method reported elsewhere.¹⁴ Cross-links were introduced at polymer concentrations 6% w/w. The average number of monomer units between neighboring cross-links (cross-linker: glutaraldehyde) was 100, and the gel is correspondingly denoted by 6/100. The samples were swollen respectively in a moderately good solvent (isopropyl alcohol at 70 °C), in a very good solvent (acetone at 25 °C), and in a Θ solvent (isopropyl alcohol at 52 °C).

Elasticity and Swelling Pressure Measurements. Measurements of the elastic modulus G were performed on isometric gel cylinders (height and diameter approximately 1 cm) prepared in a special mold. Network samples were uniaxially compressed (at constant volume) between two parallel flat plates. The stress-strain data were determined in the range of deformation ratio $0.7 < \Lambda < 1.0$.

The swelling pressure of the gels was measured using a deswelling technique described previously.^{14,15} Gel samples, placed in a dialysis bag, were equilibrated with solutions of poly(vinyl acetate) of known osmotic pressure^{16,17} in the corresponding solvent. The concentrations in both the gel and solution phases were measured by weighing.

The swelling pressure ω is the resultant of the osmotic pressure Π , which causes the network to absorb solvent, and the elastic restraining pressure, which is equal to the elastic modulus G . Thus, $\omega = \Pi - G$. In un-cross-linked semidilute solutions the osmotic pressure obeys a scaling relation of the form¹⁸

$$\Pi = A\varphi^n \quad (4)$$

where $n = 2.25$ in good solvent and $n = 3$ in Θ conditions.

Figure 1 shows the sum $\omega + G$ ($=\Pi$) for the PVAc gels swollen in isopropyl alcohol at 52 °C (squares) and in acetone (circles). In this double-logarithmic plot the sum $\omega + G$ displays an approximately straight-line behavior (dotted lines), in approximate agreement with the scaling expectation (4); in this representation the shear modulus G (crosses) also yields a straight line, whose slope is consistent with the classical behavior for elastic networks¹⁹

$$G = G_0\varphi^{1/3} \quad (5)$$

The values found for the parameters A , G_0 , and n from the least-squares fit are listed in Table 1. Although eq 4 provides a fair description for Π over the observed concentration range, good fits can also be obtained with the modified Flory-Huggins expression for a polymer solution of infinite molecular weight¹

$$\Pi = -\frac{RT}{v_1}[\ln(1 - \varphi) + \varphi + \chi\varphi^2]$$

where

$$\chi = \chi_0 + \chi_1\varphi + \chi_2\varphi^2 \quad (6)$$

and v_1 is the molar volume of the solvent. Equation 6 is

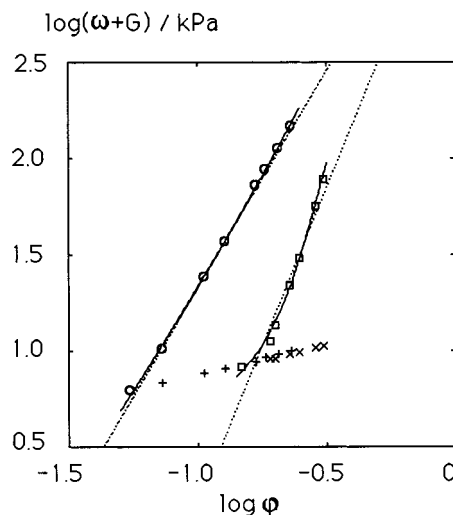


Figure 1. Shear modulus G in a 6/100 PVAc gel swollen to various degrees in acetone at 25 °C (+) and in isopropyl alcohol at 52 °C (×). In these diluents, the sum $\Pi = \omega + G$, where ω is the swelling pressure, approximately obeys a scaling relation (steep dotted lines). The corresponding scaling exponents in eq 4 are $n = 3.28$ for isopropyl alcohol (open squares) and $n = 2.28$ for acetone (open circles). The theoretically² expected values for these exponents are 3 (Θ condition) and 2.25 (excluded volume), respectively. Continuous lines are fits to the Flory-Huggins expression 6.

expected to yield a better fit than eq 4 to the data in the higher concentration range. The continuous lines in Figure 1 show the corresponding fits of eq 6 through the data points. Although the two types of fit appear to be equally good, for scattering experiments, which depend on the derivative $\partial\Pi/\partial\varphi$, such differences can become important, particularly at higher concentrations.

Small-Angle Neutron Scattering. The small-angle neutron scattering (SANS) measurements were made at the D11 and D22 instruments at the ILL Grenoble, using an incident wavelength of 10 and 8 Å, respectively. The Q range explored was $0.003 \text{ Å}^{-1} \leq Q \leq 0.19 \text{ Å}^{-1}$. Counting times of between 20 min and 2 h were used. Calibration of the scattered neutron intensity was performed using the signal from a 1 mm thick water sample in conjunction with the absolute intensity measurements of Ragnetti et al.²⁰

The sample cells were 1 mm thick quartz windows with a 1.0 mm thick Viton O-ring spacer. For the backgrounds, mixtures of protonated and deuterated solvent were prepared for which the transmission factor was as close as possible to that of the sample. The values taken for the contrast factor, calculated from the tabulated scattering lengths of the constituent nuclei²¹ and the known densities of polymer and solvent, were

$$\text{PVAc-isopropyl alcohol-}d: (\rho_p - \rho_s)^2 = 2.44 \times 10^{21} \text{ cm}^{-4}$$

$$\text{PVAc-acetone-}d: (\rho_p - \rho_s)^2 = 1.68 \times 10^{21} \text{ cm}^{-4} \quad (7)$$

The dry gels were cut into the form of flat disks and allowed to swell in the deuterated solvent in the available space within the sample cell.

Results and Discussion

Θ and Moderate Solvents. The decomposition procedure underlying eq 3 can be verified by comparing the values of M_{os} obtained from the scattering data with those calculated from the swelling pressure and elastic

Table 1. Osmotic Swelling Pressure Parameters from Eqs 4 and 6

| solvent | A/kPa | G_0/kPa | n | $RT/v_1/\text{kPa}$ | χ_0 | χ_1 | χ_2 |
|--------------|----------------|------------------|-----------------|---------------------|----------|----------|----------|
| IPA 52°C | 3180 ± 150 | 13.5 ± 2.0 | 3.28 ± 0.01 | 3.51×10^4 | 0.467 | 0.593 | -0.42 |
| acetone 25°C | 3970 ± 20 | 15.6 ± 0.7 | 2.26 ± 0.01 | 3.37×10^4 | 0.446 | 0.266 | -0.02 |

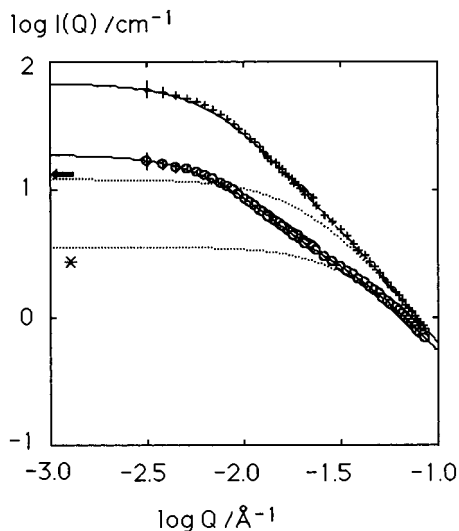


Figure 2. SANS spectra of a PVAc gel swollen in isopropyl alcohol at 52 °C (+) and at 70 °C (O). The continuous lines are the fits of eq 3 to the data, and the dotted lines are the calculated dynamic component. The arrow shows the dynamic intensity expected from swelling pressure measurements at 52 °C, same units, and the asterisk indicates the dynamic intensity obtained from quasi-elastic light scattering at 70 °C, also in the same units.

modulus measurements. From eq 6,

$$M_{\text{os}}^{\text{calc}} = \frac{RT}{v_1} \left[\frac{\varphi^2}{1-\varphi} - 2\chi_0\varphi^2 - 3\chi_1\varphi^3 - 4\chi_2\varphi^4 \right] + G_0\varphi^{1/3} \quad (8)$$

where the parameters χ_0 , χ_1 , χ_2 , and G_0 are taken from Table 1.

Figure 2 shows the SANS spectra from a PVAc gel swollen to the same degree ($\varphi = 0.148$) in isopropyl alcohol at 52 °C (Θ solvent) and at 70 °C (good solvent). The arrow on the ordinate axis shows the absolute values of the intensity $(\rho_p - \rho_s)^2(kT\varphi^2/M_{\text{os}}^{\text{calc}})$, where the contrast factor is defined in eq 7. For the observations at 70 °C the asterisk indicates the intensity found by dynamic light scattering, expressed in the same units as the SANS data.²² Given that these techniques are totally independent, the agreement between the numerical values is acceptable.

Acetone. Figure 3 shows the SANS spectra of a set of identical 6/100 PVAc gels swollen to differing degrees in acetone. The continuous curves are the fits of eq 3 to the data points. At small values of Q the fit is poor; i.e., eq 3 underestimates the scattered intensity from the gel. Although the statistical errors increase at low Q owing to the smaller number of pixels in this region of the area detector, the discrepancy lies outside the error of the measurements. It is possible that the large-scale structure yielding this extra scattering could be the result of microfissuring induced by the high swelling power of acetone. For the purposes of this article, we ignore this feature.

The arrows in Figure 3 show values of the dynamic component for each concentration calculated from eq 8,

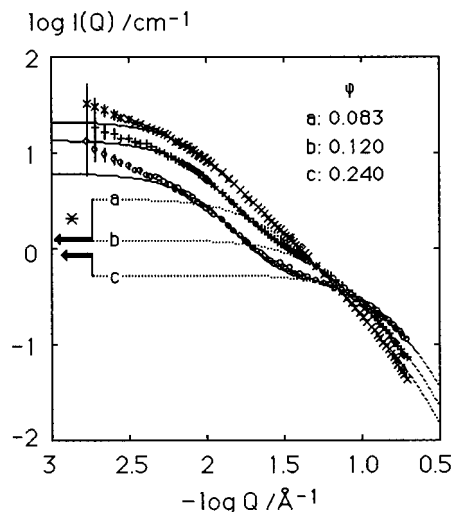


Figure 3. SANS spectra of PVAc gels swollen in acetone at 25 °C swollen to different polymer volume fractions. The continuous lines are the fits of eq 3 to the data, and the dotted lines are the calculated dynamic component. The star symbol gives the intensity of the dynamic component obtained by dynamic light scattering from the fully swollen gel (a).²¹ The arrows indicate the intensity calculated from eq 8 and the swelling pressure parameters listed in Table 1.

while the asterisk indicates that obtained from dynamic light scattering for the most swollen sample. Owing to the various factors involved, these evaluations are subject to different systematic errors. It is instructive, however, to observe that the SANS estimates of the dynamic component vary more strongly with concentration than those obtained from the swelling pressure measurements. At the higher concentrations, this result can be readily understood: extrapolations of osmotic pressure measurements tend to underestimate $\partial\Pi/\partial c$, even in un-cross-linked solutions, where no decomposition of the scattering spectra is required.¹⁶ Since the shoulder in the SANS spectra due to osmotic fluctuations is more clearly defined as the concentration increases, we therefore consider these results to be more reliable. For the most swollen gels, however, the fitting to eq 3 tends systematically to overestimate the dynamic component. The situation does not significantly improve if an additional Debye–Bueche term containing a third characteristic length is appended to eq 3. To describe gels that are fully swollen in a good solvent, it appears that the Debye–Bueche term in eq 3 must be replaced by a function that has a weaker Q dependence, such as the scaling expression used by Falcão et al.⁸ Owing to its lack of cutoff at high Q , however, this latter function is less satisfactory in describing the deswollen gels.

Uniaxial Swelling. Unfolding of the polymer chains can also be achieved through uniaxial deformation of the swollen sample, whereby the gel is stretched along one direction and compressed along the perpendicular axes.^{23,24} This situation is formally equivalent to uniaxial swelling and, in analogy with the above observation in isotropically swollen gels, should also lead to the separation of cross-links. The experimental arrangement is illustrated in Figure 4. In Figure 5 the resulting

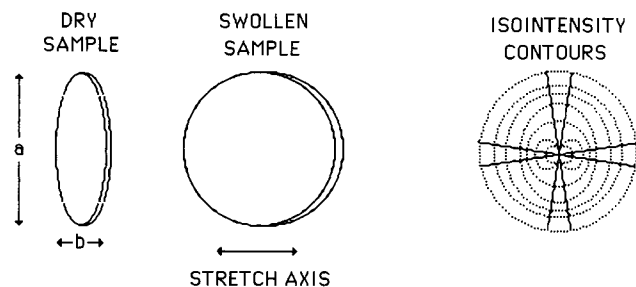


Figure 4. Experimental procedure for anisotropic measurements. Elliptical samples of aspect ratio a/b , cut from a sheet of dry network, are allowed to swell in surplus solvent inside the cylindrical sample holder. Azimuthal averages $I_{\parallel}(Q)$ and $I_{\perp}(Q)$ of the resulting anisotropic scattering figure are taken in the two orthogonal sectors shown ($\theta = \pm 0.15$ rad).

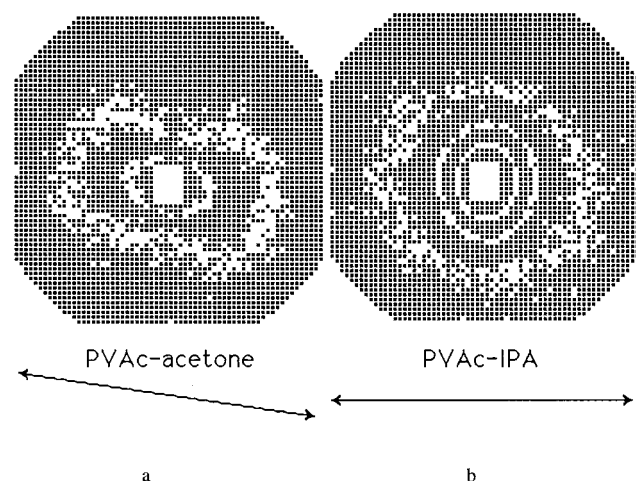


Figure 5. SANS isointensity contour patterns from a PVAc gel swollen anisotropically (a) in acetone at 25 °C to $\varphi = 0.166$ (aspect ratio $a/b = 2.5$) and (b) in isopropyl alcohol at 52 °C to $\varphi = 0.425$ (aspect ratio $a/b = 1.6$). Sample-detector distance = 20 m, $\lambda = 10$ Å, pixel area = 1 cm². Stretch axes as indicated by arrows.

isointensity contours are shown for a PVAc/acetone gel ($\varphi = 0.166$, aspect ratio $a/b = 2.5$) and for a PVAc/isopropyl alcohol gel at 52 °C ($\varphi = 0.425$, aspect ratio $a/b = 1.6$). A striking difference in behavior is visible between these two systems, in which the usual butterfly pattern^{24–27} is visible in one case and, in the other, is occulted by another effect.

We first examine PVAc/acetone. Figure 6a shows the principal components (averaged, as illustrated in Figure 4, in angular sectors of ± 0.15 rad) of the corresponding two-dimensional spectrum, along the directions parallel and perpendicular to the stretch axis. The fits of eq 3 to these two data sets show that the dynamic components have practically the same intensity in the two directions. This implies that the osmotic swelling pressure in the deformed gel is, within experimental error, isotropic. Figure 6b shows the perpendicular component of the same spectrum together with the (azimuthally averaged) spectrum of an isotropically swollen gel at a similar concentration ($\varphi = 0.154$). The two curves practically coincide, a result that is reflected in the corresponding fitting parameters listed in Table 2. For the static component, it has been previously argued²⁶ that since the swelling pressure is isotropic, then the amplitude of the second term in eq 3, divided by Ξ^3 , should also be isotropic. This parameter, expressed in Table 2 in terms of the ratio $\langle \delta \varphi^2 \rangle / \varphi^2$, varies

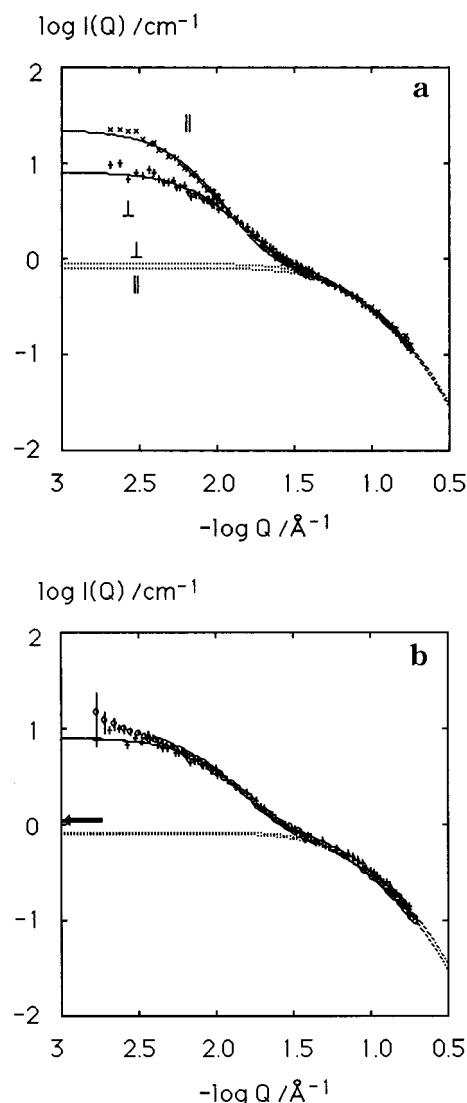


Figure 6. (a) Parallel and perpendicular components, $I_{\parallel}(Q)$ (\times) and $I_{\perp}(Q)$ ($+$), of the scattered intensity for the PVAc/acetone sample of Figure 5a. Continuous lines are least-squares fits to eq 3, the dotted curves being the dynamic term. Parameters of these fits are listed in Table 2. (b) Perpendicular component of the scattered intensity $I_{\perp}(Q)$ for the PVAc/acetone sample in Figure 5a at $\varphi = 0.166$ ($+$) and spectrum of isotropically swollen sample at $\varphi = 0.154$ (\circ). Parameters of the least-squares fits shown are listed in Table 2. Arrow indicates dynamic scattering intensity for a theoretical gel of concentration $\varphi = 0.16$, calculated from eq 8.

by less than 10% between the two directions, in support of the observations of ref 26.

For the case of PVAc/isopropyl alcohol at the Θ condition, the situation appears to be different. In Figure 7 are shown the two principal components of the spectrum, $I_{\parallel}(Q)$ and $I_{\perp}(Q)$, for the sample of Figure 5b. In both these figures a faint butterfly pattern can just be discerned in the vicinity of $Q \approx 0.01$ Å⁻¹ (i.e., the isointensity pattern is slightly elongated in the stretch direction), but this effect is dwarfed at small Q by a much more intense feature exhibiting the opposite tendency. In the same figure is shown the spectrum of a similar PVAc/isopropyl alcohol gel swollen isotropically to approximately the same concentration ($\varphi = 0.408$). The spectra from these samples are qualitatively dissimilar and cannot be analyzed in the same way by means of eq 3. In the double-logarithmic representation of Figure 7 the feature at lowest Q in

Table 2. Scattering Parameters from Fits to Eq 3 (Solvent: Acetone)

| φ | $(\rho_p - \rho_s)^2 (kT\varphi^2/M_{os})/\text{cm}^{-1}$ | $(\rho_p - \rho_s)^2 8\pi\Xi^3 \langle \delta\varphi^2 \rangle / \text{cm}^{-1}$ | $\xi/\text{\AA}$ | $\Xi_1/\text{\AA}$ | $\langle \delta\varphi^2 \rangle / \varphi^2$ |
|-------------------|---|--|------------------|--------------------|---|
| 0.083 | 3.3 ± 0.1 | 18.1 ± 0.2 | 43.4 ± 0.6 | 89.5 ± 0.9 | 0.087 |
| 0.120 | 1.22 ± 0.01 | 12.4 ± 0.1 | 21.4 ± 0.1 | 85.8 ± 0.5 | 0.032 |
| 0.154 | 0.80 ± 0.01 | 7.2 ± 0.1 | 15.4 ± 0.1 | 75.6 ± 0.4 | 0.017 |
| 0.166 \parallel | 0.80 ± 0.04 | 21.5 ± 1.2 | 14.5 ± 0.4 | 120 ± 3 | 0.011 |
| 0.166 \perp | 0.83 ± 0.04 | 7.2 ± 0.4 | 14.0 ± 0.4 | 79 ± 2 | 0.012 |
| 0.240 | 0.51 ± 0.01 | 5.62 ± 0.05 | 11.1 ± 0.1 | 76.7 ± 0.4 | 0.005 |

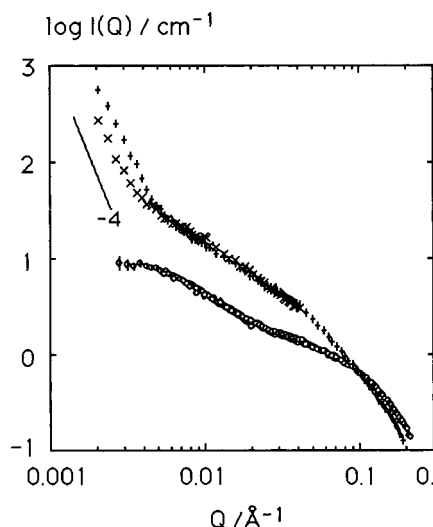


Figure 7. Scattering spectra from PVAc samples swollen in isopropyl alcohol at 52 °C: circles, gel swollen isotropically at $\varphi = 0.408$ for the PVAc/isopropyl alcohol sample in Figure 5b; \times , $I_{\parallel}(Q)$; $+$, $I_{\perp}(Q)$.

the anisotropic case has a slope of approximately -3.5 , for both parallel and perpendicular components. When allowance is made for the residual signal from the rest of the sample, this observation is consistent with regions of the sample displaying a Porod Q^{-4} behavior,²⁸ characteristic of phase separation. In Figure 7 the ratio of the intensity of this feature along the two directions, $I_{\perp}(Q)/I_{\parallel}(Q)$, is in excess of 2. Porod's law states that the product IQ^4 is proportional to the interfacial area connecting the phase-separated regions. From Figure 7 it follows therefore that the interfacial area perpendicular to the stretch direction is at least twice that for the parallel direction; i.e., the precipitate particles deform along the stretch direction, and more strongly than the overall sample ($a/b = 1.6$). These precipitated regions must therefore be softer than the rest of the sample and probably correspond to solvent-rich regions (formed due to partial phase separation).

The spectrum of the stretched sample in Figure 7 is also instructive in that, outside the Porod region, the scattering intensity for $Q \leq 0.1 \text{ \AA}^{-1}$ is significantly enhanced over that of the isotropically swollen gel. This result shows that mechanical deformation shifts the swelling equilibrium toward poorer solvent conditions and is consistent with the partial phase separation observed in the Porod region.

Conclusion

The present SANS observations were made on PVAc gels swollen in solvents of differing quality. In samples swollen isotropically in a Θ solvent (IPA at 52 °C) and in moderately good solvent conditions (isopropyl alcohol at 70 °C), as well as in the excellent solvent acetone, the gel spectra are reasonably described by two length

scales: the thermodynamic correlation length ξ , which is analogous to the correlation length in semidilute polymer solutions, and a static correlation length Ξ , related to the local elastic constraints. The former depends both on concentration and on the quality of the solvent, while the second varies weakly with degree of swelling. For the PVAc gels swollen anisotropically in acetone, analysis of the resulting butterfly pattern using this separation procedure shows that the effects of the osmotic pressure remain isotropic. At high degrees of swelling the separation procedure employed still works but appears to overestimate the intensity of the dynamic component.

For gels stretched uniaxially in Θ solvent conditions, incipient phase separation is observed, in which the precipitated particles are elongated along the macroscopic stretch direction. Their mechanical response suggests that these particles are soft, probably solvent-rich regions in the partially phase-separated gel.

Acknowledgment. We are grateful for neutron beam time on the D11 and D22 instruments at the ILL, Grenoble. We also acknowledge Grant OTKA T016872 from the Hungarian Academy of Sciences.

References and Notes

- (1) Flory, P. J. *Principles of Polymer Chemistry*; Cornell University Press: Ithaca, NY, 1953.
- (2) de Gennes, P. G. *Scaling Concepts in Polymer Physics*; Cornell University Press: Ithaca, NY, 1979.
- (3) Ferry, J. D. *Viscoelastic Properties of Polymers*; Wiley: New York, 1980.
- (4) Mallam, S.; Hecht, A.-M.; Geissler, E.; Pruvost, P. *J. Chem. Phys.* **1989**, *91*, 6447–6454.
- (5) Soni, V. K.; Stein, R. S. *Macromolecules* **1990**, *23*, 5257–5265.
- (6) Bastide, J.; Leibler, L.; Prost, J. *Macromolecules* **1990**, *23*, 1821–1825.
- (7) Horkay, F.; Hecht, A. M.; Mallam, S.; Geissler, E.; Rennie, A. R. *Macromolecules* **1991**, *24*, 2896–2902.
- (8) Falcão, A. N.; Pedersen, J. S.; Mortensen, K. *Macromolecules* **1993**, *26*, 5350–5364.
- (9) Benoit, H.; Higgins, J. *Neutron Scattering from Polymers*; Oxford University Press: Oxford, 1994.
- (10) Geissler, E.; Horkay, F.; Hecht, A. M.; Rochas, C.; Lindner, P.; Bourgaux, C.; Couarraze, G. *Polymer* **1997**, *38*, 15–20.
- (11) Landau, L. D.; Lifshitz, E. M. *Statistical Mechanics*, 2nd ed.; Pergamon Press: Oxford, 1969.
- (12) Tanaka, T.; Hocker, L. O.; Benedek, G. B. *J. Chem. Phys.* **1973**, *59*, 5151–5159.
- (13) Debye, P.; Bueche, R. M. *J. Appl. Phys.* **1949**, *20*, 518–525.
- (14) Horkay, F.; Zrinyi, M. *Macromolecules* **1982**, *15*, 1306–1310.
- (15) Nagy, M.; Horkay, F. *Acta Chim. Acad. Sci. Hung.* **1980**, *104*, 49–61.
- (16) Horkay, F.; Hecht, A.-M.; Stanley, H. B.; Geissler, E. *Eur. Polym. J.* **1994**, *30*, 215–219.
- (17) Vink, H. *Eur. Polym. J.* **1974**, *10*, 149–156.
- (18) Horkay, F.; Hecht, A. M.; Geissler, E. *J. Chem. Phys.* **1989**, *91*, 2706–2711.
- (19) Treloar, L. R. G. *The Physics of Rubber Elasticity*, 3rd ed.; Clarendon Press: Oxford, 1975.
- (20) Ragnetti, M.; Geiser, D.; Höcker, H.; Oberthür, R. C. *Makromol. Chem.* **1985**, *186*, 1701–1709.
- (21) Sears, V. F. *Neutron News* **1992**, *3* (3), 26–37.

- (22) Horkay, F.; Burchard, W.; Hecht, A. M.; Geissler, E. *Macromolecules* **1993**, *26*, 4203–4207.
- (23) Geissler, E.; Duplessix, R.; Hecht, A. M. *Macromolecules* **1983**, *16*, 712–713.
- (24) Rouf, C.; Bastide, J.; Pujol, J. M.; Schosseler, F.; Munch, J. P. *Phys. Rev. Lett.* **1994**, *73*, 830–833.
- (25) Oeser, R. Polymer Motion in Dense Systems. *Springer Proc. Phys.* **1988**, *29*, 104.
- (26) Geissler, E.; Horkay, F.; Hecht, A. M. *J. Chem. Phys.* **1995**, *102*, 9129–9132.
- (27) Ramzi, A.; Zielinski, F.; Bastide, J.; Boué, F. *Macromolecules* **1995**, *28*, 3570–3587.
- (28) Porod, G. *Kolloid-Z.* **1951**, *124*, 83–114.

MA971606J